ORIGINAL PAPER

Experimental and Numerical Study of Strip Footing Supported on Stabilized Sand Slope

M. El Sawwaf

Abstract The paper presents the results of laboratory model tests and theoretical analysis on the behavior of a strip footing supported on sheet pile wall-stabilized sandy slope and loaded vertically to failure. The parameters varied in the study include the height, stiffness and location of the sheet pile wall, the location of the footing relative to the slope crest and the relative density of sand. Two-dimensional plane strain finite element analyses was used to analyze a prototype strip footing on sandy slope with same conditions. The results indicate that the inclusion of sheet pile wall has significant effect in improving the response of the strip footing and the slope itself. The theoretical results confirm the experimental results of the model footing tests and show reasonable agreement. Based on the numerical and experimental results, critical values of the sheet pile wall parameters for maximum stabilizing effect are established.

Keywords Strip footing · Sheet pile · Slope · Bearing capacity · Finite element analysis

1 Introduction

There are many situations where shallow footings are constructed on sloping surfaces or adjacent to a slope crest such as footings for bridge abutments on sloping embankments. When a footing is located on a sloping ground, not only the bearing capacity of the soil may be significantly reduced, but also the potential failure of the slope itself significantly increased depending on the location of the footing with respect to the slope. Therefore, over years, the subject of stabilizing earth slope has become one of the most interesting areas for scientific research and attracted a great deal of attention. Typical examples include modifying the slope surface geometry, chemical grouting, using soil reinforcement, or installing continuous or discrete retaining structures such as diaphragm walls, sheet pile walls or piles.

Several studies on the effect of using soil reinforcement to stabilize soil slope on bearing capacity behavior of a footing constructed adjacent to the slope have been reported (Selvadurai and Gnanendran 1989; Sawicki and Lesniewska 1991; Mandal and Labhane 1992; Huang et al. 1994; Zornberg et al. 1998; Yoo 2001; El Sawwaf 2007). These investigations have demonstrated that not only the slope stability can be increased but also both the ultimate bearing capacity and the settlement characteristics of the foundation can be significantly improved by the inclusion of reinforcements (layers of geogrid, strips or geotextile) in the earth slope. On the other hand, the use of stabilizing piles to support active earth slope has been considered to be one of the important slope reinforcement techniques in the last few decades. These piles, which can be driven at

M. El Sawwaf (✉)
Faculty of Engineering, Tanta University, Tanta, Egypt
e-mail: Mos_sawaf@hotmail.com

the crest or within the slope itself act as resisting members and are usually subjected to lateral forces by the horizontal movements of the surrounding soil. Several studies reported the successful use of piles in many situations in order to improve slope stability (De Beer and Wallays 1970; Viggiani 1981; Poulos 1995; Lee et al. 1995; Hong and Han 1996; Chen and Poulos 1997; Hassiotis et al. 1997; Hull and Poulos 1999; Ausilio et al. 2001).

Sheet pile walls are also used for retaining earth slopes, excavation and as temporary supports in foundation construction. Sheet pile walls resist the overturning moment due to pressure from the retained soil by developing a restraining moment due to passive pressure at the base along the embedment length of the wall. Several studies reported experimental data and suggested design guidelines (King 1995; Bowles 1996; Sivakumar Babu and Munwar Basha 2008). The focus of these studies was on the design procedures of sheet pile wall and determining the penetration depth required to satisfy equilibrium of moments and horizontal forces. However, to the best knowledge of the author, the behavior of a footing constructed adjacent to slope stabilized using sheet pile wall or diaphragm walls has not been investigated. Therefore, the aim of this study is to gain more understanding about the mechanical behavior and the failure mechanism of a strip footing supported on sand bed adjacent to sheet pile stabilized earth slope both experimentally and theoretically. The main objective was to determine and establish the relationship between the variable parameters of a sheet pile and the bearing capacity of the footing. Also, to find out the best location of the sheet pile that gives the best improvement in the footing bearing capacity.

2 Laboratory Model Tests

2.1 Model Box, Footing and Sheet Pile Wall

The test box, having inside dimensions of 1.0 m × 0.5 m in plan and 0.5 m in depth is made from steel with the front wall made of 20 mm thickness glass and is supported directly on two steel columns as shown in Fig. 1. These columns are firmly fixed in two horizontal steel beams, which are firmly clamped in the lab ground using four pins. The
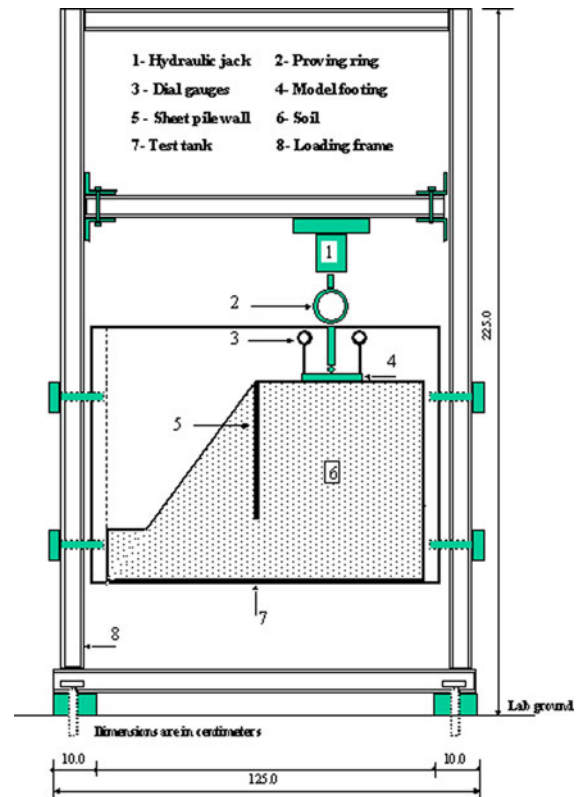
Fig. 1 Schematic view of the experimental apparatus

glass side allows the sample to be seen during preparation and sand particle deformations to be observed during testing. The tank box was built sufficiently rigid to maintain plane strain conditions by minimizing the out of plane displacement. To ensure the rigidity of the tank, the back wall of the tank was braced on the outer surface with two steel beams fitted horizontally at equal spacing. The inside walls of the tank are polished smooth to reduce friction with the sand as much as possible by attaching fiber glass onto the inside walls.

A plane strain footing was used in the study while a sheet pile wall was used to stabilize the earth slope. A model strip footing made of steel with a hole at its top center to accommodate a bearing ball was used. The footing was 498 mm in length, 80 mm in width and 20 mm in thickness. The footing was positioned on the sand bed with the length of the footing running the full width of the tank. The length of the footing was made almost equal to the width of the tank in order to maintain plane strain conditions. The two ends of the footing plate were polished smooth to

minimize the end friction effects. A rough base condition was achieved by fixing a thin layer of sand onto the base of the model footing with epoxy glue.

The loading system was mounted by a horizontal SIB steel beam supported on the two columns. It consists of a hand-operated hydraulic jack and pre-calibrated load ring. The load is transferred to the footing through a bearing ball as shown in Fig. 1. Such an arrangement produced a hinge, which allowed the footing to rotate freely as it approached failure and eliminated any potential moment transfer from the loading fixture. Model sheet pile walls made of aluminium with different heights and thickness were used in the study. The walls were 80.0, 160.0, 240, 320, and 400 mm in height and 3, 6, 10 mm in thickness.

2.2 Test Material

The sand used in this research was medium to coarse sand, washed, dried and sorted by particle size. It was composed of rounded to sub-rounded particles. The sand had a very low impurity level with a quartz (SiO_2) content of 97%. The specific gravity of the soil particles was determined by the gas jar method. Three tests were carried out producing an average value of 2.65. The maximum and the minimum dry densities of the sand were found to be 19.95 and 16.34 kN/m^3 and the corresponding values of the minimum and the maximum void ratios were 0.31 and 0.59, respectively. The particle size distribution was determined using the dry sieving method and the results are shown in Fig. 2. The effective size (D_{10}), uniformity coefficient (C_u), and coefficient of curvature (C_c) for the sand were 0.15 mm, 4.07 and 0.77, respectively.
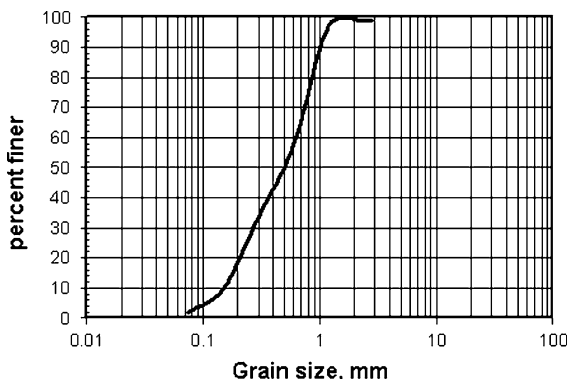

Fig. 2 Grain size distribution of the used sand

Controlled pouring and tamping techniques were used to deposit sand in 50 mm thick layers into the model box. In this method the quantity of sand for each layer, which was required to produce a specific relative density, was first weighed and placed in the tank and tamped until achieving the required layer height. The experimental tests were conducted on samples prepared with average unit weights of 17.44, 18.15 and 19.10 kN/m^3 representing loose, medium-dense and dense conditions, respectively. The relative densities of the samples were 35, 55 and 80%, respectively. The estimated internal friction angle of the sand determined from direct shear tests using specimens prepared by dry tamping at the same relative densities were 34°, 37.5° and 43° respectively.

Once setting up of sand slope was completed, a sheet pile wall was installed using a special guide system which holds the sheet pile vertical during the installation. The guide system was initially clamped in the tank edges and then the sheet pile was pushed vertically by hand at the design location. No visible movement in sand slope was observed during the installation process. The difference in the relative density of the sand which occurs during sheet pile wall installation due to the difference in the sheet pile heights or thickness was considered to be small and neglected.

2.3 The Experimental Setup and Test Program

Model soil slopes with a height of 440 mm were constructed in layers with the bed level observed through the front glass wall. The sand was set up to form a slope of 3 (H): 2 (V). In pouring the last layer, the sand top surface was approximately horizontal and the sand slope was about the required inclination. Great care was given to level the top surface of the sand and the slope face using special straight edges so that the relative density of the top layer was not affected. The model sheet pile wall and the footing were placed on position and the load was applied incrementally by the hydraulic jack until reaching failure. Each load increment was maintained constant till the footing settlements had stabilized. These settlements were measured using two 0.001 mm accuracy dial gauges, placed on opposite sides across the center of the footing.

A total of 50 tests in twelve series were carried out. Each series was intended to study the effect of
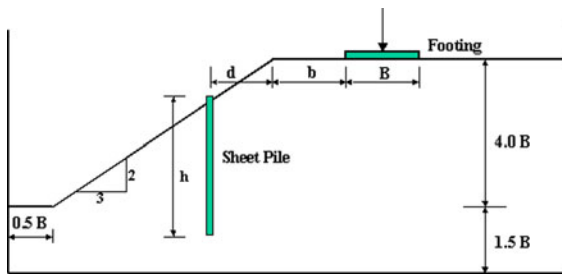
Fig. 3 Geometric parameters of sheet pile-stabilized sand slope model

one parameter while the other variables were kept constant. Initially, the behavior of non-stabilized sand slopes made at different densities and loaded by model footing placed at different location of the slope edge was determined (series 1–3). Then, four series of tests were performed to study the effect of the sheet pile height (h) and the best location of the sheet pile from the slope crest (d) that gives the maximum bearing capacity as shown in Fig. 3. Then three series of tests (8–10) were conducted to find out the effect of the footing location (b) on the behavior of stabilized sand slope made at different relative density (R_d). Finally the effect of sheet pile wall stiffness was studied by varying the thickness of the sheet pile wall (T_{sp}). Table 1 summaries all the tests programs with both the constant and varied parameters illustrated. Several tests were repeated at least twice to verify the repeatability and the consistency of the test data.

3 Prototype Study

3.1 Finite Element Analysis

A series of two-dimensional nonlinear finite element analysis on a prototype plane strain footing-slope system was performed to verify the laboratory model tests results and understand the deformation trends within the soil mass. The analysis was performed using the finite element program Plaxis, version 7 (Bringkgreve and Vermeer 1998). Plaxis is capable of handling a wide range of geotechnical problems such as deep excavations, tunnels, and earth structures such as retaining walls and slopes. A prototype footing was assumed to rest on the surface of sandy soil adjacent to slope having the same inclination of model test slopes 3 (H): 2 (V). The geometry of the prototype footing-slope system was assumed to be 10 times the laboratory model (the footing width $B = 80$ cm and footing thickness, $t = 20$ cm, soil height $= 440$ cm). The same properties of sand and the material of sheet pile wall were used in the prototype study.

3.2 Finite Element Modeling

The non-linear behavior of sand was modeled using the hardening soil model, which is an elastoplastic hyperbolic stress–strain model, formulated in the framework of friction hardening plasticity. The foundation and the sheet pile wall were treated as elastic beam elements based on Mindlin's beam

Table 1 Model tests programs

Series	Constant parameters	Variable parameters
1	Non-stabilized slope, $R_d = 80\%$	$b/B = 0.0, 1.0, 2.0, 3.0, 4.0$
2	Non-stabilized slope, $R_d = 55\%$	$b/B = 0.0, 1.0, 2.0, 3.0, 4.0$
3	Non-stabilized slope, $R_d = 35\%$	$b/B = 0.0, 1.0, 2.0, 3.0, 4.0$
4	$b/B = 0.0, d/B = 0, R_d = 80\%, T_{SP} = 6.0$ mm	$h/B = 1.0, 2.0, 3.0, 4.0, 4.5$
5	$b/B = 2.0, d/B = 0, R_d = 80\%, T_{SP} = 6.0$ mm	$h/B = 1.0, 2.0, 3.0, 4.0, 4.5$
6	$b/B = 0, h/B = 3.0, R_d = 80\%, T_{SP} = 6.0$ mm	$d/B = 0.0, 1.0, 1.5, 2.0, 3.0$
7	$b/B = 0, h/B = 3.0, R_d = 55\%, T_{SP} = 6.0$ mm	$d/B = 0.0, 1.0, 1.5, 2.0, 3.0$
8	$h/B = 4.0, d/B = 0, R_d = 80\%, T_{SP} = 6.0$ mm	$b/B = 0.0, 1.0, 2.0, 3.0, 4.0$
9	$h/B = 4.0, d/B = 0, R_d = 55\%, T_{SP} = 6.0$ mm	$b/B = 0.0, 1.0, 2.0, 3.0, 4.0$
10	$h/B = 4.0, d/B = 0, R_d = 35\%, T_{SP} = 6.0$ mm	$b/B = 0.0, 1.0, 2.0, 3.0, 4.0$
11	$b/B = 0, h/B = 3.0, d/B = 0, R_d = 80\%$	$T_{SP} = 3.0, 6.0, 10.0$
12	$b/B = 1, h/B = 3.0, d/B = 0, R_d = 80\%$	$T_{SP} = 3.0, 6.0, 10.0$

B is the footing width; b is the distance between the footing and the slope crest; h is the sheet pile depth

d is the distance between sheet pile and the slope crest; R_d is the relative density; T_{sp} is the thickness of the sheet pile wall

theory with significant flexural rigidity (EI) and normal stiffness (EA). The interaction between the sheet pile wall and soil is modeled at both sides by means of interface elements, which allow for the specification of a reduced wall friction compared to the friction of the soil. A basic feature of the hyperbolic model is the stress dependency of soil stiffness. The limiting state of stress are described by means of the secant Young's modulus (E_{50}^{ref}), Poisson's ratio (v), effective cohesion (c), angle of internal friction (ϕ), and interface reduction factor (R_{int}). A refined mesh was adopted to minimize the effect of mesh dependency on the finite element modeling of cases involving changes in the height, thickness, and the location of sheet pile wall. A prescribed footing load was then applied in increments (load control method) accompanied by iterative analysis up to failure.

The effect of the height, location and stiffness of sheet pile wall, the location of the footing relative to the slope crest along with the sand relative density on the behavior of the footing have been investigated. As the slope surface is not horizontal, the gravity loading was applied to calculate the initial stress field of the soil in steps with the sheet pile wall in place. Automatic generation of 15 node triangle plane strain elements for the soil, five node beam elements for the footing and the sheet pile wall were used. The boundary conditions were chosen such that the vertical boundaries are free vertically and constrained horizontally while the bottom horizontal boundary is fully fixed. The analyzed prototype slope geometry, generated mesh, sheet pile wall and the boundary conditions are shown in Fig. 4. An internal angle of friction and secant Young's modulus representing,
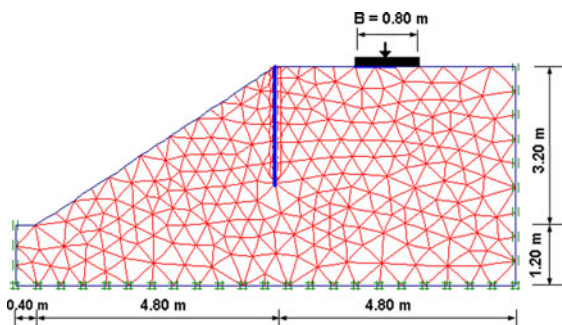
Fig. 4 The prototype slope geometry, generated mesh, and boundary conditions

loose, medium dense and dense sand conditions derived from a series of drained triaxial compression tests were used for the sand. The hyperbolic parameters for the sand were taken from data base provided by the software manual as shown in Table 2.

4 Results and Discussion

The effects of using sheet pile walls of different heights, stiffness, and locations on the stability of sand slope and hence on the response of a strip footing at different locations of the slope crest were studied experimentally and theoretically (FEA). The bearing capacity improvement of the footing due to slope stabilization is represented using a non-dimensional factor, called bearing capacity ratio factor (BCR). This factor is defined as the ratio of the footing ultimate pressure with the slope stabilized ($q_{u\ stabilized}$) to the footing ultimate pressure in tests without slope stabilizing (q_u). The footing settlement (S) is also expressed in non-dimensional form in terms of the footing width (B) as the ratio (S/B, %). The ultimate bearing capacities of the footing are determined from the load-displacement curves as the pronounced peaks, after which the footing collapses and the load decreases. In curves, which did not exhibit a definite failure point, the ultimate load is taken as the point at which the slope of the load settlement curve first reach zero or steady minimum value (Vesic 1973).

Typical variations of bearing capacity pressure (q) with settlement ratio (S/B) for a strip footing supported on dense sand bed adjacent to both stabilized and non-stabilized earth slopes are shown in Figs. 5 and 6. Measured results from model tests are plotted in Fig. 5, while results of prototype footing obtained by FEA are plotted in Fig. 6. In both series, the footing position ($b/B = 0$), the sheet pile wall location ($d/B = 0$) and the sand density ($R_d = 80\%$) were kept constant except the height of the sheet pile wall was varied. The behavior of the footing placed on non-stabilized sand slopes is included in the figures for comparison. The figures show that the installation of sheet pile wall much improves the bearing capacity load for stabilized cases compared to the non-stabilized slopes. Comparing the curves across the dotted line for the same level of settlement ratio in Fig. 5, the figure illustrates

Table 2 Hardening soil model parameters used in the finite element analysis

Parameter	Dense sand	Medium dense sand	Loose sand	Footing	Sheet pile wall
Secant Young's modulus, E_{50}^{ref}, kN/m^2	40,000	30,000	15,000	–	–
Cohesion (c), kN/m^2	1.0	0.5	0.0	–	–
Friction angle (ϕ)	40.00	35.0	31.5	–	–
Soil unit weight (γ), kN/m^3	19.10	18.15	17.44	–	–
Poisson's ratio, v	0.3	0.28	0.25	–	–
Interface reduction factor (R_{int})	0.80	0.80	0.80	–	–
E (kN/m^2)	–	–	–	2.10×10^8	0.70×10^8

PLAXIS can handle cohesionless sands ($C = 0.0$) but to avoid complications, values of 1.0, 0.5 and 0.0 for dense, medium dense and loose sand as given in the software manual were used

that the inclusion of sheet pile wall improved the bearing capacity from 20.3 kPa for non-stabilized case to 33.1 kPa when using sheet pile with $h/B = 4$. Also, it can be seen that the settlement ratio decreases with increasing the sheet pile height for the same footing pressure. However, greater sheet pile heights results in increasing the settlement ratio at failure. The curves show that the mode of failure is a general shear failure in which a pronounced peak can be observed in the load settlement curve, after which the footing collapses and the load decreases. Comparing Figs. 5 and 6, it can be seen that the general trends of FEA are similar to those of the model footing. Both figures confirm the significant increase in the bearing capacity of the footing with the increase of the sheet pile height. The measured and calculated ultimate loads for footing supported on both stabilized and non-stabilized sand slopes for the different studied parameters are given in Tables 3, 4, 5, 6, 7, and 8.

These results for each parameter are discussed in the following sections.

4.1 The Effect of Sheet Pile Wall Height

Ten model tests along with ten numerical studies in four series were carried out to determine the sheet pile height that give the optimum response of the footing. Figure 7 shows comparisons of the measured BCR from the model tests and the calculated BCR from the finite element analysis of prototype slope (FEA) for the different sheet pile heights and footing positions. The curves demonstrate the same pattern of footing response for the different sheet pile heights. The BCR increases with the increase of h/B for the two footing positions. However, this improvement in the ultimate bearing capacity with increasing sheet pile height is significant until a value of ($h/B = 3$)
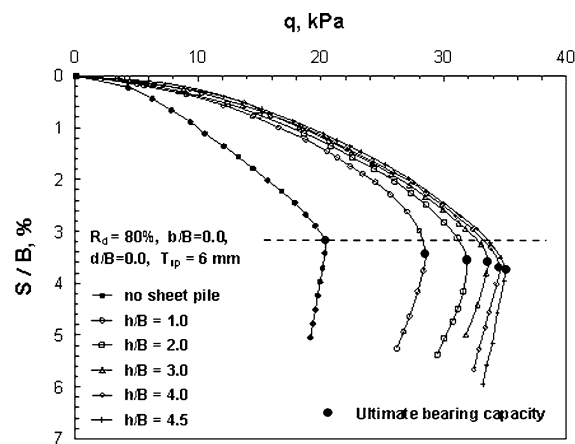
Fig. 5 Variations of bearing pressure (q) with settlement ratio (S/B) for model footing for different sheet pile depths
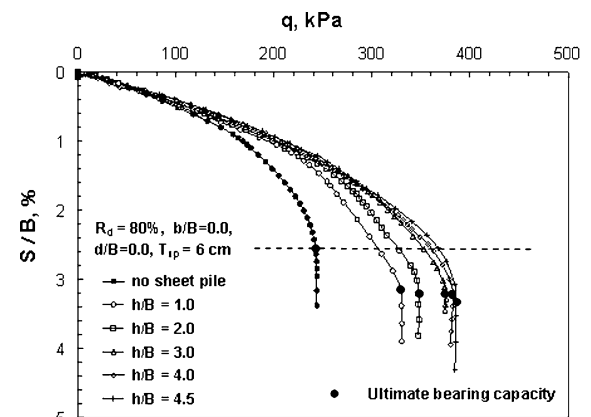
Fig. 6 Variations of bearing pressure (q) with settlement ratio (S/B) for prototype footing for different sheet pile heights (FEA)

Table 3 Results of footings supported on dense sand at different (b/B) ratios

Test results	Non stabilized					Stabilized				
	b/B					b/B				
	0	1. 0	2.0	3.0	4.0	0	1. 0	2.0	3.0	4.0
q (kPa) model	20.3	38.8	112.5	213.5	235.6	34.53	58.84	157.96	285.34	310.44
q (kPa) FEA	242.0	410.5	593.9	853.8	859.7	382.8	579.6	805.4	1061.4	1068.7

Table 4 Results of footings supported on medium dense sand at different (b/B) ratios

Test results	Non stabilized					Stabilized				
	b/B					b/B				
	0	1. 0	2.0	3.0	4.0	0	1. 0	2.0	3.0	4.0
q (kPa) model	11.4	19.66	44.65	102.34	134.75	18.46	27.89	58.94	130.5	170.22
q (kPa) FEA	93.5	199.4	314.2	423.1	437.5	143.7	268.7	398.7	513.3	523.8

Table 5 Results of footings supported on loose sand at different (b/B) ratios

Test results	Non stabilized					Stabilized				
	b/B					b/B				
	0	1. 0	2.0	3.0	4.0	0	1. 0	2.0	3.0	4.0
q (kPa) model	4.45	7.68	22.32	42.4	50.1	6.78	10.24	26.62	48.48	57.74
q (kPa) FEA	24.6	75.0	143.4	239.7	240.7	35.70	95.0	161.8	258.0	259.6

Table 6 Results of footings supported on dense sand with different h/B and b/B Ratios

Test results	b/B = 0.0					b/B = 2.0				
	h/B					h/B				
	1. 0	2.0	3.0	4.0	4.5	1. 0	2.0	3.0	4.0	4.5
q (kPa) model	28.5	31.88	33.61	34.53	34.64	126.94	138.24	153.16	157.96	160.3
q (kPa) FEA	329.0	347.5	375.3	382.8	385.8	6,829	706.5	775.5	805.4	811.5

**Table 7** Results of footings supported on sand slope with different R_d and d/B Ratios

Test results	R_d = 80%					R_d = 55%				
	d/B					d/B				
	0	1. 0	1.5	2.0	3.0	0	1. 0	1.5	2.0	3.0
q (kPa) model	33.61	30.98	28.24	25.62	24.64	17.88	16.3	14.7	13.46	13.2
q (kPa) FEA	375.3	354.3	318.2	292.2	286.8	142.2	129.6	118.7	107.9	106.1

beyond which further increase in height of sheet pile does not show significant contribution in increasing the ultimate load of the footing. Using a sheet pile with (h/B = 4) placed at slope crest resulted in improvements in the bearing capacity as great as 1.70 and 1.40 times those of the non-stabilized cases for

Table 8 Results of footings supported on sand slope with different b/B and T_{SP}

Test results	b/B = 0.0			b/B = 1.0		
	T_{SP}			T_{SP}		
	3.0	6.0	10.0	3.0	6.0	10.0
q (kPa) model	30.5	33.61	34.4	51.46	57.54	58.25
q (kPa) FEA	342.4	375.3	380.7	514.1	575.0	597.6
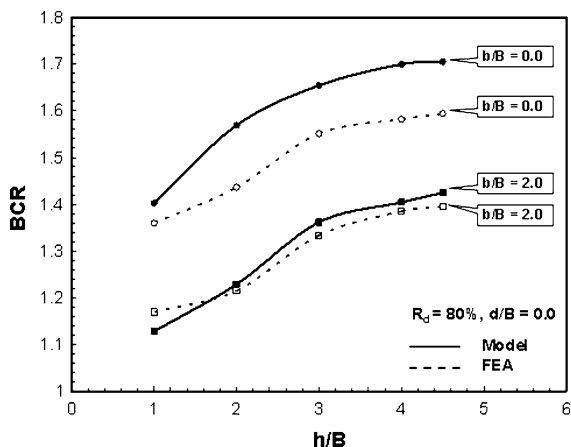
Fig. 7 Variations of bearing capacity ratio (BCR) with normalized sheet pile depth (h/B) for different footing locations

the two footing positions ($b = 0$ and $b = B$). The curves also, clearly demonstrate good agreement in the general trend of behavior of both the experimental and numerical analysis. However, the agreement between the measured and calculated values is much better when the footing is placed away of the slope crest $b/B = 2.0$ than that when is placed at the crest where the difference in the BCR values appear to be high. This difference between the model tests results and FEA calculations may be attributed to the scale effects. Inclusion of sheet pile walls had a greater effect on the footing response when it was located at slope crest than that when placed away of the crest. The same trend can be seen in both model and FEA studies.

This improvement in footing behavior can be attributed to the stability effect of the sheet pile wall to the slope, which limits the spreading and lateral deformations of sand particles towards the slope. Increasing sheet pile height results in greater sheet pile stability due to the increase of the embedded part of the sheet pile deeper underlying soils and hence

yields less rotation of the sheet pile and soil lateral deformations. However, when the footing is placed far from the crest ($b/B = 2$), the passive resistance is relatively large and the contribution of the sheet pile to the bearing capacity improvement is reduced.

4.2 The Effect of the Sheet Pile Location

Two series of model tests along with two series of numerical studies were conducted to investigate the optimum location of the sheet pile that gives the maximum bearing capacity improvement for footing. Sand beds set up at medium dense and dense conditions along with sheet pile walls of the same height ($h/B = 3.0$) at five different locations relative to the slope crest were used. Figure 8 shows the variations of BCR of the footing with the location of the sheet pile wall for both model and prototype slope. The figure show the significant effect of inclusion of the sheet pile when it was placed at slope crest relative to any other location. The closer is the sheet pile to the slope crest the greater is improvement in the bearing capacity. The same trend is observed for tests carried out using different sand densities. The curves also show that the general trends obtained from the theoretical analysis are in good agreement with those measured from the model tests although the values of BCR from the model slope appears to be slightly greater than that from the FEA.

This conclusion that the most effective sheet pile location in terms of the bearing capacity of a footing is at the slope crest can be related to the fact that the
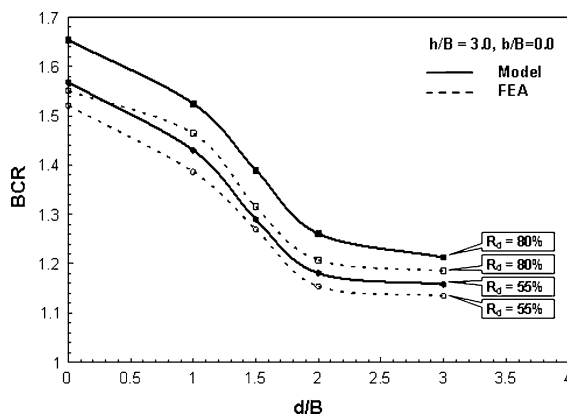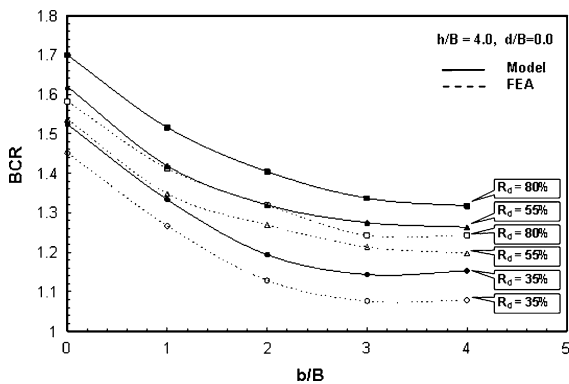

Fig. 8 Variations of bearing capacity ratio (BCR) with normalized sheet pile location (d/B) for different sand densities

passive wedge under the footing is relatively shallow. Therefore, when the sheet pile is placed closer to the slope crest it interrupts the failure surface and resists the lateral displacements of soil particles and hence, the mobilized passive resistance increases. Other sheet pile positions may increase the overall stability of the slope itself but did not intersect with failure plane and hence cannot prevent or decrease the lateral deformations of soil particles under the footing and near the slope.

4.3 The Effect of Footing Location Relative to Slope Crest

In order to study the effect of the proximity of a footing to the slope crest (b/B), six series of model tests were carried out on strip footing resting on sand slope made with loose, medium dense and dense relative densities. While the first three series were carried out on non-stabilized sand slope, the other three series were performed on sheet pile-stabilized sand slope. Same series of tests were carried out on prototype footing at the same conditions using FEA. The variation of the BCR against (b/B) ratios for both model and prototype results are plotted in Fig. 9. While Table 5 shows that the footing bearing capacities significantly decrease as the footing location moves closer to the slope crest, Fig. 9 shows that the BCR significantly increases. Also, the figure clearly shows that the maximum benefit of slope stability using sheet pile is obtained when footing is placed at slope crest. The same trend can be observed for both model and prototype slopes. As the footing location moves away from crest, the rate of decrease in BCR
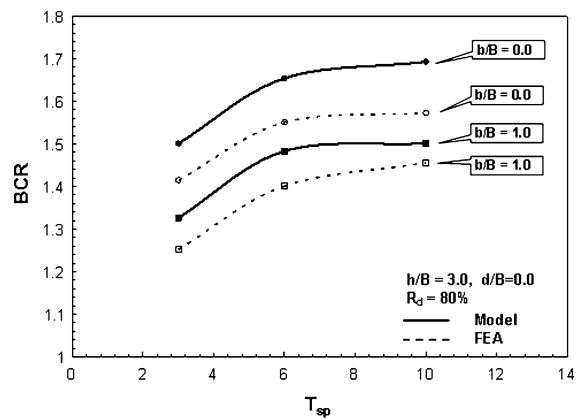
of the footing become less until a value of about $b/B = 2.5$ after which the change can be considered insignificant. The curves clearly show good agreement in the general trend of behavior of both the experimental and numerical analysis.

This change in bearing capacity of the footing with its location relative to slope crest can be attributed to soil passive resistance from the slope side and sheet pile wall effect. When, the footing is placed far away of the slope, the passive resistance from the slope side to the failure wedge under the footing increases. Moreover, using sheet pile wall resists the lateral displacements and results in wider and deeper failure zone as discusses in previous sections, leading to increasing the bearing capacity load. However, the inclusion of the sheet pile is significant for the footing response when the footing is placed near to the crest and that effect decreases as the distance between the footing and the slope crest increases.

4.4 The Effect of Sheet Pile Stiffness

In order to investigate the effect of sheet pile stiffness on the footing performance, sheet pile walls made with different thickness were used. Figure 10 shows the variations of BCR with the wall thickness (T_{sp}) for two different footing locations. The figure clearly shows that the footing performance much improves with the increase in sheet pile stiffness. However, it is clear that the rate of increase in the BCR significantly decreased with the increase of sheet pile thickness from 6 to 10 mm. Same trend can be seen for both
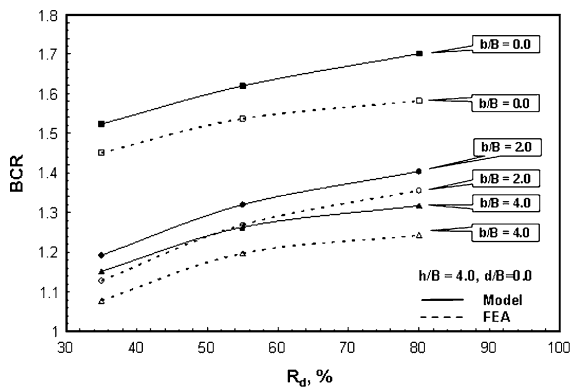

Fig. 9 Variations of bearing capacity ratio (BCR) with normalized footing location (d/B) for different sand densities

Fig. 10 Variations of bearing capacity ratio (BCR) with normalized sheet pile thickness (T_{sp}) for different footing locations
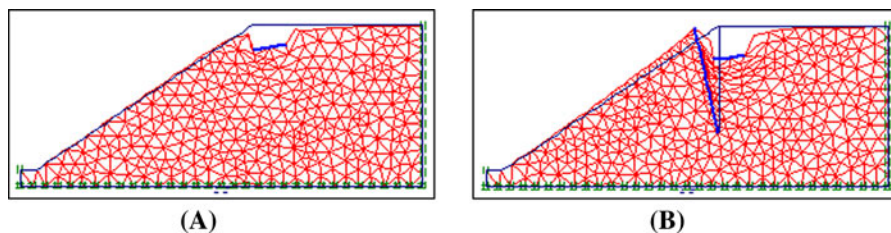
model and prototype footings. Increasing of sheet pile thickness resulted in increase in the sheet pile stiffness leading to greeter resistance to the lateral displacements of soil particles underneath the footing and hence improving in the bearing capacity. However, the effectiveness of the sheet pile stiffness is dependent on its location relative to the footing and its stability as discussed in the previous sections.

4.5 The Effect of the Relative Density

In order to study the effect of relative density, six series of tests were conducted on footings supported on sand samples with three unit weights representing loose, medium dense and dense relative densities. The changes in the BCR for model and prototype footing placed at different locations from the slope crest are plotted against the relative density in Fig. 11. The figure clearly shows that the sheet pile wall is very effective in improving the ultimate bearing load of footings supported on medium dense to dense sands more than that of footings on loose sands. Also, it can be seen that for the same relative

density, the BCR increases as distance between the footing and the slope crest decreases. This increase in footing resistance with relative density can be attributed to the increase in the angle of friction of the sand and hence leading to greater bearing capacity.

4.6 Displacement Vectors and Failure Mechanism

Figure 12 compares the failure pattern and deformed mesh for prototype strip footing placed at the crest of both non-stabilized and sheet pile-stabilized sand slope. Figure 12a clearly shows the footing rotation and settlement toward the slope face, which cause significant reduction in the footing bearing capacity. Comparing figures a and b it can be seen that the inclusion of sheet pile, results in increasing the settlement ratio at failure which is consistent with the observed behavior from the experimental tests that the improvement in the bearing capacity is accompanied with an increase in the settlement ratio. However, both figures a and b show that the footing failure is accompanied by tilting and tendency to move toward the slope face without any potential failure in the slope itself. In order to understand the mechanism of footing failure experimentally and whether or not it was accompanied with slope failure, additional increments of loads were applied after failure point (the pronounced peak in the load–settlement readings) and both the footing and the slope were observed through the front glass wall. It was noticed that, as the footing approached failure, the vertical settlements were accompanied with horizontal movements and rotations (toward the slope). It is very important to mention that in all the experimental tests, failure was not observed in the slope itself even after footing settlement S/B ratio reached 50%.

Fig. 11 Variations of bearing capacity ratio (BCR) with sand relative density (R_d) for different footing locations

Fig. 12 Failure pattern and deformed FE mesh for prototype footing on sand slope; **a** non-stabilized slope; **b** stabilized slope

Figure 13 shows typical plots of the displacement vectors obtained from FEA under prototype footing supported on the non-stabilized and stabilized earth slopes. The observed displacement vectors at failure for the stabilized slope are widely distributed underneath the footing for greater width and depth along the sheet pile face than that in the non-stabilized case which are concentrated underneath the footing toward the slope face. The plastic flow clearly demonstrates that the sheet pile wall resist the particle deformations toward the slope face and push them downward for deeper depth and width which in turn results in a longer failure surface and greater bearing capacity.

5 The Effect of Sheet Pile Inclusion on Slope Stability

When a sheet pile wall is inserted in a slope, the additional resistance provided by these sheet piles changes both the slope safety factor and potential failure mechanism with respect to the case without sheet pile. Figure 14 shows a sandy slope assuming a planar slip surface inclined at an angle (α) to the horizontal. A planer surface was assumed for simplicity of calculation although considerable evidence suggests that the slope failure usually occurs on curved surface. The factor of safety (F_S) of case without sheet pile can be derived by:

$$F_S = \tan\phi / \tan\alpha \tag{1}$$

In order to estimate the factor of safety of the stabilized slope, the lateral force (SP_{LR}) that the sheet pile wall can resist is initially determined. The shear strength of the slip surface can be defined by the friction angle (ϕ) while the shear stress can be define by the slip surface inclination angle (α). The factor of safety (F_S) of the case with sheet pile is derived by:

$$\begin{aligned} F_S &= \text{Resisting Forces/Driving Force} \\ &= \{(W\cos\alpha)\tan\phi + SP_{LR}\}/W\sin\alpha. \end{aligned} \tag{2}$$

Equation 2 demonstrates the dependence of the F_S on the lateral capacity of the sheet pile which depends on its strength, stiffness and stability. While increasing the sheet pile thickness increases its stiffness, increasing sheet pile height results in greater sheet pile stability and hence resistance to lateral loads and therefore greater factor of safety of slope.

6 Scale Effects

The model footing adopted in laboratory study was reduced to a certain scale while the used sand was the same in the model and the prototype analysis. Therefore, the response of the model footing or the soil may not be the same as the behavior of the prototype and it might cause some influence on the experimental results, which is called scale effects

Fig. 13 Displacement vectors plot for prototype footing on sand slope; **a** non-stabilized slope; **b** stabilized slope
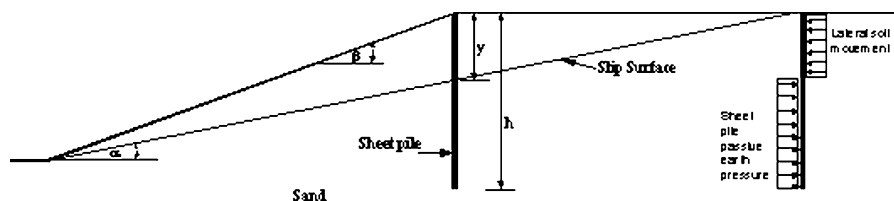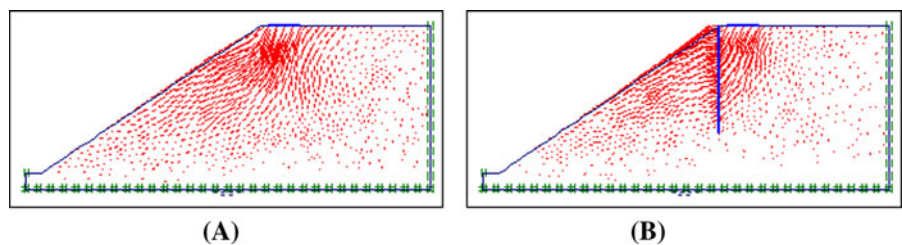
Fig. 14 Sheet pile interruption of wedge slope failure

(Vesic 1973; Steenfelt 1977). These differences occur primarily because of the differences in stress level between the model tests and the field tests and the influence of the footing width/grain size ratio. The second effect vanishes provided particle size is small compared to the footing dimension. However, scaling effects due to variations in stress level will occur in 1 g (earth gravity) modeling. Therefore, due to scale effects, the results of model footing may be influenced and cause differences in the data when compared with prototype analysis.

7 Conclusions

An experimental and numerical study of the behavior of strip footing supported on sandy slope with and without sheet pile wall are presented. The effects of the inclusion of sheet pile walls of different height, stiffness, and location along with the location of the footing relative to the slope crest and the relative density of sand were investigated. Based on the laboratory tests and the theoretical analysis, the following main conclusions are drawn:

1. Stabilizing earth slope using a sheet pile wall has a significant effect in improving the bearing capacity of a strip footing supported on granular soil adjacent to the slope crest. However, the maximum benefit obtained from the inclusion of sheet pile wall is dependent on the sheet pile stiffness and location.
2. Increasing sheet pile height resulted in increasing the embedded part deeper underlying soils and hence the stability of the sheet pile leading to improvement in BCR. For the studied problem and condition, the recommended h/B ratio is ($h/B \geq 3$).
3. In terms of bearing capacity improvement rather than the overall stability of the slope itself, the optimal location of the sheet pile wall is at the slope crest.
4. The improvement on the footing performance is dependent on the footing location relative to slope crest. Sheet pile is most effective when the footing is placed closer to the slope and the effect of the slope on the footing response may be neglected once the footing is placed a distance of more than 2.5 times the footing width from the slope crest.
5. A close agreement between the experimental and numerical results relative to trend of behavior and the critical values of the studied parameters is observed. In all cases, the BCR obtained from the model results appears to be greater than that calculated from the FEA.

References

Ausilio E, Conte E, Dente G (2001) Stability analysis of slopes reinforced with piles. Comput Geotech 28:591–611

Bowles JE (1996) Foundation analysis and design, 5th edn. The McGraw-Hill Book Company, Singapore

Bringkgreve R, Vermeer P (1998) PLAXIS-finite element code for soil and rock analysis. Version 7. PLAXIS, The Netherlands

Chen LT, Poulos HG (1997) Piles subjected to lateral soil movements. J Geotech Geoenviron Eng 123(9):802–811

De Beer E, Wallays M (1970) Stabilization of a slope in schist by means of bored piles reinforced with steel beams. In: Proceedings of the 2nd international congress on rock mechanics, Beograd

El Sawwaf M (2007) Behavior of strip footing on geogrid-reinforced sand slope over soft clay. Geotext Geomembr 25(1):50–60

Hassiotis S, Chameau J, Gunaratne M (1997) Design method for stabilization of slopes with piles. J Geotech Geoenviron Eng ASCE 123(4):314–323

Hong WP, Han JG (1996) The behavior of stabilizing piles installed in slopes. In: Proceedings of the 7th international symposium on landslides, Rotterdam, pp 1709–1714

Huang C, Tatsuoka F, Sato Y (1994) Failure mechanisms of reinforced sand slopes loaded with a footing. Soils Found 24(2):27–40

Hull TS, Poulos HG (1999) Design method for stabilization of slopes with piles. J Geotech Geoenviron Eng ASCE 125(10):911–913

King GJW (1995) Analysis of cantilever sheet pile walls in cohesionless soil. J Geotech Eng ASCE 121(9):629–635

Lee C, Hull T, Poulos H (1995) Simplified pile-slope stability analysis. Comput Geotech 17:1–16

Mandal J, Labhane L (1992) A procedure for the design and analysis of geosynthetic reinforced soil slopes. Geotech Geol Eng 10(4):291–319

Poulos HG (1995) Design of reinforcing piles to increase slope stability. Can Geotech J 32(5):808–818

Sawicki A, Lesniewska D (1991) Stability of fabric reinforced cohesive soil slopes. Geotext Geomembr 10:125–146

Selvadurai A, Gnanendran C (1989) An experimental study of a footing located on a sloped fill: influence of a soil reinforcement layer. Can Geotech J 26(3):467–473

Sivakumar Babu G, Munwar Basha B (2008) Optimum design of cantilever sheet pile walls in sandy soils using inverse reliability approach. Comput Geotech 35:134–143

Steenfelt JS (1977) Scale effect on bearing capacity factor (N_γ). In: Proceedings of the IXth international conference in soil mechanics and foundation engineering, Tokyo, vol 1, pp 749–752

Vesic AS (1973) Analysis of ultimate loads of shallow foundations. J Soil Mech Found Div ASCE 94((SM3)):661–688

Viggiani C (1981) Ultimate lateral load on piles used to stabilize landslides. In: Proceedings of the 10th international conference on soil mechanics and foundation engineering, Stockholm, pp 555–560

Yoo C (2001) Laboratory investigation of bearing capacity behavior of strip footing on geogrid-reinforced sand slope. Geotext Geomembr 19:279–298

Zornberg J, Sitar N, Mitchell J (1998) Performance of geosynthetic reinforced slopes at failure. J Geotech Geoenviron Eng 124(8):670–683